Modeling Turbulent Flow Velocity Profiles in Irregularly shaped Open Channels: A 3D Approach

Kamel Benoumessad

Laboratory of Applied Research in Hydraulics, Department of Hydraulics, Faculty of Technology, University of Batna 2, Batna, Algeria
Kamel.benoumessad@univ-batna2.dz (corresponding author)

Fatima Zohra Fourar

Department of French, University of Khenchela, Algeria
fourar.fatimazohra@univ-khenchela.dz

Ali Fourar

Laboratory of Applied Research in Hydraulics, Department of Hydraulic, Faculty of Technology, University of Batna 2, Batna, Algeria
a.fourar@univ-batna2.dz

Fawaz Massouh

Ecole National Superieure d'Arts et Metiers, Paris, France
fawaz.massouh@ensam.eu

ABSTRACT

Numerically simulating turbulent open-channel flows represents a formidable challenge in *C*omputational *F*luid *D*ynamics (CFD), particularly when addressing the interplay of transient turbulence, irregular bathymetry, and dynamic free-surface interactions inherent to natural river systems. This study advances a three-dimensional nonlinear (k-ε) turbulence model to resolve flow dynamics, velocity distributions, and mass transport mechanisms in both meandering and straight open channels. The framework leverages cylindrical coordinate systems to accommodate curvilinear geometries, enabling precise representation of intricate channel boundaries. *The g*overning equations are discretized *with* the finite volume method, with pressure-velocity coupling achieved through the SIMPLE algorithm. The nonlinear (k-ε) formulation is uniquely suited to capture anisotropic turbulence effects while maintaining computational efficiency, addressing a critical gap in conventional isotropic eddy-viscosity models. Key innovations include the development of a geometrically adaptive numerical framework capable of simulating flow in meandering channels with variable curvature and width-to-depth ratios. Parametric analys*i*s reveal*s* that secondary circulations, driven by curvature-induced centrifugal forces and bed roughness heterogeneity, profoundly influence *the* velocity profiles and scalar transport. The model successfully predicts flow separation at bends, velocity-dip phenomena beneath free surfaces, and pollutant dispersion patterns in compound channels. Validations against empirical datasets confirm the model's fidelity in replicating turbulent kinetic energy distributions and Reynolds stress anisotropy. This *study* establishes the nonlinear (k-ε) model as a versatile tool for analyzing hydraulically complex environments, including sediment-laden rivers and vegetated wetlands. By integrating geometric adaptability with advanced turbulence closures, the framework bridges theoretical CFD advancements and practical applications in flood risk mitigation, eco-hydraulic engineering, and contaminant transport modeling. The findings underscore the necessity of resolving anisotropic turbulence and secondary flow mechanisms to achieve predictive accuracy in real-world, geometrically heterogeneous open-channel systems.

Keywords-simulation; velocity profile; open channels; numerical modeling; CFD; nonlinear turbulence; k-ε model; finite volume method; anisotropy; complex boundaries

I. INTRODUCTION

The numerical modeling of flow in curved open channels represents a critical and intricate challenge in river engineering, particularly for discharge estimation and flood risk management. Accurate simulation of these flows is hindered by the interplay of centrifugal forces and shear effects, which dominate channel bends. While laboratory experiments yield essential insights into flow behavior, they are often resource-intensive, time-consuming, and difficult to extrapolate to real-world conditions. Nevertheless, experimental datasets remain indispensable for calibrating and validating numerical models, which are pivotal for achieving precise simulations. Early modeling efforts for curved channels relied on simplified one-dimensional (1D) or two-dimensional (2D) frameworks based on the Saint-Venant equations. These approaches assume uniform velocity profiles and hydrostatic pressure distributions, oversimplifications that fail to capture the depth-dependent and transverse variations in velocity and pressure inherent to curved geometries.

A foundational advancement was introduced by the authors in [1], who developed a quasi-three-dimensional (3D) model incorporating a logarithmic vertical distribution of the longitudinal velocity while retaining the hydrostatic pressure assumption. Tested in a 180° curved channel, this model enabled rudimentary 3D flow analysis. Authors in [2] expanded this work by proposing a depth-averaged 2D model that simulated velocity distributions using parabolic profiles, though still constrained by hydrostatic assumptions. Secondary flows, critical to redistributing velocity and pressure in channel bends, were later addressed through advanced modeling techniques. Authors in [3] enhanced existing frameworks by integrating dispersion stress terms to account for secondary flow effects and authors in [4] further refined these methods with a vertically averaged model incorporating adaptive velocity and pressure distributions, improving the representation of bend-induced hydrodynamic complexity. Direct Numerical Simulations (DNS) and Large-Eddy Simulations (LES) have advanced the resolution of open-channel flow dynamics. However, many implementations impose rigid free-surface boundary conditions (e.g. [5]), neglecting vertical surface motions. Authors in [6] employed linearized boundary conditions to approximate free-surface behavior, while the LES studies in [7-10] adopted similar rigid-surface assumptions to leverage methodologies developed for internal flows. To address moving boundaries, techniques such as the Volume of Fluid (VOF) method [11] and the hybrid VOF approaches with split-merge capabilities [12] have been developed, enabling accurate free-surface tracking. Authors in [13] further contributed a subgrid scale model to analyze surface motion dynamics and their filtering effects.

In this study, we present a 3D numerical model based on the Reynolds-Averaged Navier-Stokes (RANS) equations coupled with the $(k-\varepsilon)$ turbulence closure. This framework resolves vertical velocity and pressure distributions while capturing secondary flow effects in curved open channels. Validation against experimental data ensures the model's robustness for practical applications in hydraulic engineering and environmental fluid dynamics.

II. GOVERNING EQUATIONS AND MODELING HYPOTHESIS

A 3D, unsteady, and free-surface viscous flow is assumed. The pressure is decomposed into a hydrostatic component and a hydrodynamic component. The Reynolds-averaged Navier-Stokes and continuity equations are expressed by:

$$\frac{\partial u_i}{\partial t} + \frac{\partial u_i \partial u_j}{\partial x_j} - \nu \frac{\partial^2 u_i}{\partial x_j \partial x_j} + \frac{1}{\rho}\frac{\partial \tau_{ij}}{\partial x_j} + \frac{1}{\rho}\frac{\partial p}{\partial x_i} + g\delta_{i3} = 0 \quad (1)$$

$$\frac{\partial u_i}{\partial x_i} = 0 \quad (2)$$

where t represents time, u_i is the i-th component of the Reynolds averaged velocity, x_i is the i-th axis (with the axis x_3 being vertical and oriented upward), ρ is the water density, p is the Reynolds averaged pressure, g is the acceleration due to gravity, v is the kinematic viscosity, δ_{ij} is the Kronecker delta, and T_{ij} represents the Reynolds stresses.

The Reynolds Averaged Navier-Stokes equations can be rewritten as:

$$\frac{\partial u_i}{\partial t} + \frac{\partial u_i \partial u_j}{\partial x_j} - \nu \frac{\partial^2 u_i}{\partial x_j \partial x_j} + \frac{1}{\rho}\frac{\partial \tau_{ij}}{\partial x_j} +$$
$$+ \frac{1}{\rho}\frac{\partial q}{\partial x_i} + g\frac{\partial(z_B + h)}{\partial x_i} = 0 \quad (3)$$

where z_B is the bed elevation from a horizontal plane of reference $z = 0$, h is the water column depth, and q is the non-hydrostatic pressure.

The turbulent stresses (τ_{ij}) are computed using the $(k-\varepsilon)$ turbulence model. Turbulent quantities, including turbulent kinetic energy (k) and dissipation rate (ε), are derived from their respective transport equations, enabling dynamic evaluation of free-surface evolution over time [9].

$$\tau_{ij} = -\rho \nu_t \left(\frac{\partial u_i}{\partial x_j} + \frac{\partial u_j}{\partial x_i} \right) + \frac{2}{3}\delta_{ij}k \quad (4)$$

with:

$$\nu_t = c_\mu k^2 / \varepsilon \quad (5)$$

where ν_t is the eddy viscosity. The turbulent kinetic energy and the dissipation rate are obtained from:

$$\frac{\partial k}{\partial t} + \frac{\partial u_i k}{\partial x_j} = \frac{\partial}{\partial x_j}\left(\frac{\nu_t}{\partial k}\frac{\partial k}{\partial x_j} \right) + P - \varepsilon \quad (6)$$

$$\frac{\partial \varepsilon}{\partial t} + \frac{\partial u_i \varepsilon}{\partial x_j} = \frac{\partial}{\partial x_j}\left(\frac{\nu_t}{\partial \varepsilon}\frac{\partial \varepsilon}{\partial x_j} \right) + (c_{\varepsilon 1}P - c_{\varepsilon 2}\varepsilon)\frac{\varepsilon}{k} \quad (7)$$

where P is the production of the turbulent kinetic energy given by:

$$P = \nu_t \left(\frac{\partial u_i}{\partial x_j} + \frac{\partial u_j}{\partial x_i} \right)\frac{\partial u_i}{\partial x_j} \quad (8)$$

The free surface movements are calculated according to the kinematic condition:

$$\frac{\partial h}{\partial t} + u_1 \frac{\partial(h + z_B)}{\partial x_1} + u_2 \frac{\partial(h + z_B)}{\partial x_2} - u_3 = 0 \qquad (9)$$

Equations (9), (3) allow calculating the free surface position at each time step. These equations develop a complete hydrodynamic model able to represent flow.

Compared to earlier frameworks [1, 2] the present model employs full 3D resolution, capturing longitudinal and transverse velocity variations as functions of depth with enhanced precision. Furthermore, it addresses limitations inherent to LES and DNS approaches by integrating moving boundary conditions via VOF and subgrid-scale methods, significantly improving adaptability for practical simulations.

Recent studies [14] have applied coupled CFD and Discrete Element Method (DEM) frameworks to analyze fluid-particle interactions in curved channels. This CFD-DEM coupling proves effective for modeling sediment transport in bends and predicting erosion-deposition zones. Meanwhile, modern LES implementations incorporate free and mobile boundary conditions, enabling improved representation of surface fluctuations and wave effects critical for sediment transport and mass exchange processes. Authors in [15] demonstrated the efficacy of the Lattice Boltzmann Method (LBM) in resolving free-surface flows within complex geometries, capturing interfacial dynamics and secondary flows without velocity profile approximations. LBM's inherent parallelizability also positions it as a viable candidate for high-resolution simulations.

Advancements in Artificial Intelligence (AI) have spurred the development of predictive models for curved-channel flows, such as the neural network-based frameworks in [16]. While these machine learning models enable real-time discharge forecasting, their accuracy may diminish for channel configurations absent from training datasets.

III.   NUMERICAL APPLICATION

To numerically resolve the governing equations outlined in the preceding section, custom boundary conditions were applied across the computational domain. A no-slip condition was imposed at the lateral walls and channel bed to accurately model viscous fluid behavior, while atmospheric pressure was prescribed at the free surface to maintain hydrostatic equilibrium. At the domain boundaries, water surface elevation and velocity profiles were explicitly defined. Zero normal derivatives were enforced at the outlet for all dependent variables to ensure numerical stability and physically consistent outflow. Inlet boundary conditions were derived from a prior simulation of flow in a straight channel, leveraging periodic boundary conditions in the longitudinal direction. This approach ensures seamless initialization of flow variables while preserving mass and momentum conservation. The curved channel features a rectangular cross-section with a width of 1 m, height of 0.6 m, and total length of 16 m. A central curvature radius of 2 m was implemented to facilitate analysis of bend-induced flow dynamics. This configuration enables detailed interrogation of flow behavior in complex geometries, particularly for elucidating shock wave dynamics and secondary flow interactions. The numerical framework

provides critical insights into flow phenomena in curved channels, with applications spanning hydraulic engineering and environmental fluid mechanics. By resolving 3D velocity gradients and free-surface deformations, the model advances predictive capabilities for scenarios involving rapid flow transitions and sediment transport.

IV.   DISCUSSION

The results highlight critical dynamic features of flow within the curved channel, where velocity profiles and secondary circulation vectors reveal distinct flow patterns. As illustrated in Figures 1, 2, and 3(a–b), secondary currents exhibit a downward migration toward the inner bank near the channel bed, while near the free surface, these currents shift toward the outer bank. This bidirectional circulation drives transverse fluid transport with reduced longitudinal momentum in the central region of the channel, thereby attenuating surface velocity. The observed reduction in surface velocity, coupled with a velocity maximum immediately below the surface, is attributed to the interplay between secondary circulations and boundary effects. Air-water interfacial friction and surface flow resistance attenuate near-surface velocities, while the absence of obstructions in subsurface regions facilitates accelerated flow. Consequently, peak velocities occur at depths where kinetic energy is optimized, underscoring the pivotal role of secondary circulations in governing flow dynamics.

These findings elucidate the mechanisms by which secondary currents influence sediment transport and velocity stratification. Fine particulate matter is preferentially mobilized in high-velocity subsurface zones, while surface flow dynamics are modulated by air-water momentum exchange. The resulting velocity gradients and secondary flow structures suggest that sediment redistribution in curved channels is strongly coupled to three-dimensional hydrodynamic processes. This underscores the necessity of incorporating secondary circulation effects in predictive models for sediment transport, erosion-deposition patterns, and habitat heterogeneity in riverine systems. Figure 2 illustrates the velocity vectors in distinct regions of the channel, providing a detailed visualization of the spatial distribution, direction, and magnitude of secondary flow structures. These vector plots enable a rigorous analysis of localized hydrodynamic behavior, particularly the interplay between centrifugal forces and shear-driven momentum transfer, which governs the formation and evolution of secondary currents in curved open-channel geometries.
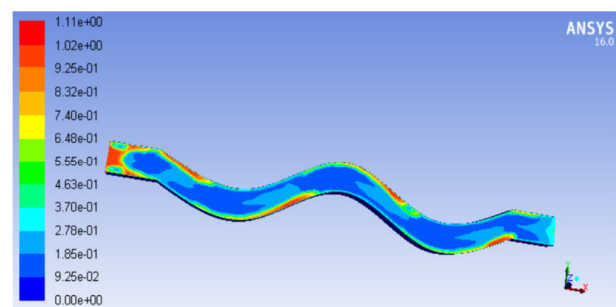
Fig. 1.   Contours of velocity magnitude (m/s).
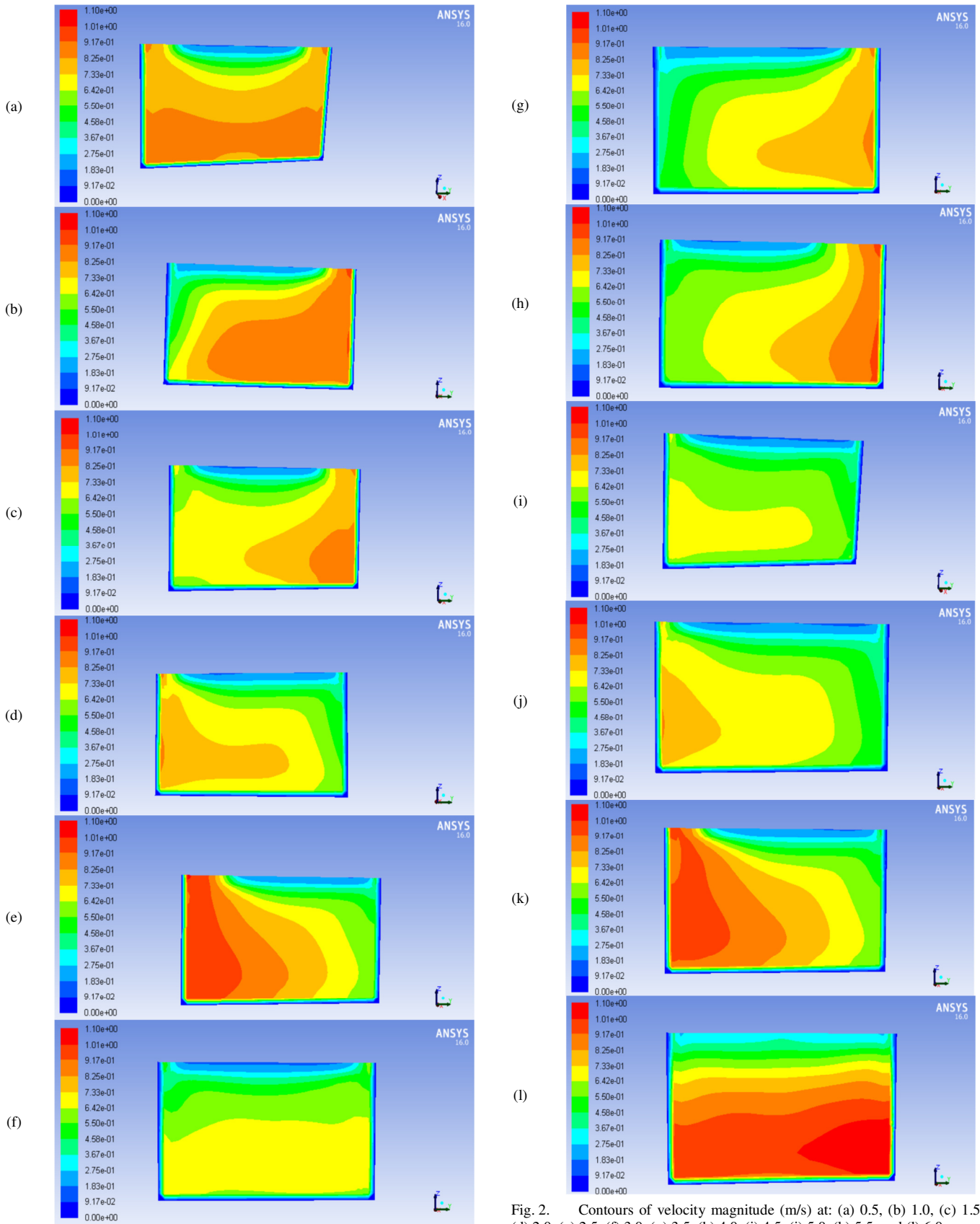
Fig. 2.   Contours of velocity magnitude (m/s) at: (a) 0.5, (b) 1.0, (c) 1.5, (d) 2.0, (e) 2.5, (f) 3.0, (g) 3.5, (h) 4.0, (i) 4.5, (j) 5.0, (k) 5.5, and (l) 6.0 m.

Figures 3-5 characterize the spatial distribution of Turbulent Kinetic Energy (TKE), turbulence intensity, and turbulent viscosity within the channel. In the curved section, the primary flow initially migrates toward the inner bank before undergoing centrifugal-driven redirection toward the outer bank. The free surface exhibits a pronounced rotational displacement, marked by elevation near the outer wall and depression near the inner wall. This deformation arises from the interplay of secondary circulations and transverse pressure gradients, which dominate momentum redistribution in the bend. The observed turbulence metrics further corroborate the role of secondary currents in modulating energy dissipation and shear stress anisotropy, critical for understanding flow stability and sediment transport dynamics in curved open-channel systems.

(a)

(b)

Fig. 3.   Contours of turbulent kinetic energy K (m^2/s^2).
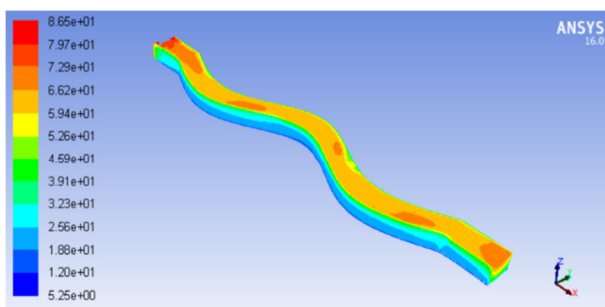
Fig. 4.   Contours of turbulent Intensity (%).

The non-uniform energy distribution along the channel shows significant dependence on local curvature and pressure variations. Pressure gradients induced by channel topography drive inward-directed secondary currents, while inertial forces arising from centrifugal effects associated with flow curvature generate outward-directed flow structures, as evidenced in Figures 5 and 6. This dynamic interplay between pressure-driven and inertia-dominated mechanisms governs the formation of secondary flow patterns, reflecting the competing influence of transverse momentum transfer and flow curvature on hydrodynamic equilibrium.
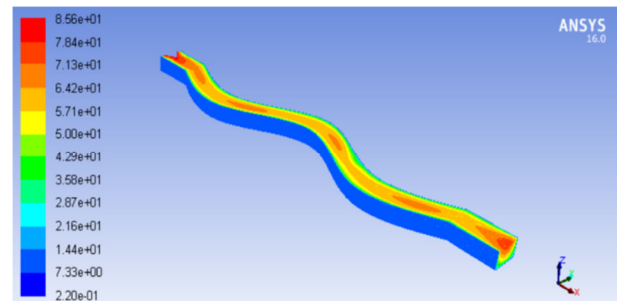
Fig. 5.   Contours of turbulent viscosity (kg/m.s).
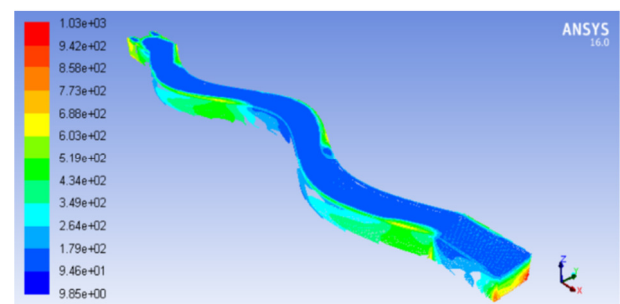
Fig. 6.   Contours of dynamic pressure (Pa).

V.   CONCLUSION AND FUTURE DIRECTIONS

This study advances the fundamental understanding of flow dynamics in curved open-channel systems by elucidating the mechanisms through which channel geometry and pressure gradients govern velocity profile asymmetries and turbulent kinetic energy distribution [15-17]. The findings hold significant implications for hydraulic engineering applications, where precise prediction of secondary flow structures and pressure-driven momentum transfer is critical for sediment transport management and flow optimization in natural and engineered aquatic systems. By quantifying the interplay between centrifugal forces and topographically induced pressure fields, this study provides actionable insights for the informed design and management of hydraulic infrastructure in fluvial and urban environments.

The numerical investigation of flow dynamics in a curved channel conducted in this study elucidates phenomena intrinsic to hydrodynamic behavior in curvilinear geometries. Through the implementation of rigorously defined boundary conditions and high-fidelity modeling of inlet/outlet domains, the derived velocity and turbulence profiles align closely with theoretical predictions for curved open-channel flows.

The results underscore the pivotal role of secondary currents, which govern both depth-dependent velocity stratification and the subsurface velocity maximum observed immediately below the free surface. This behavior emerges from the synergistic interplay of channel geometry [18-19],

inertial forces, and transverse pressure gradients collectively dictating momentum redistribution in bend regions.

Secondary circulation patterns further demonstrate pronounced influence on flow stability and sediment transport mechanisms. The concentration of kinetic energy beneath the surface, coupled with air-water interfacial friction attenuating surface velocities, directly governs sediment mobilization in natural environments [20], where bank morphology and in-stream obstacles modulate flow pathways [21].

The developed numerical framework provides granular insights into curved-channel hydrodynamics, particularly the spatial heterogeneity of turbulent energy distribution. Observed variations in turbulence intensity and dynamic pressure profiles reveal how geometric constraints amplify secondary motions, a finding with direct relevance to sediment management strategies and the design of hydraulic infrastructure [22, 23, 24]. These outcomes establish a robust foundation for future studies aimed at optimizing hydraulic conveyance systems through physics informed control of secondary flow phenomena.

The presented 3D numerical model provides a robust solution for simulating curved-channel hydrodynamics. However, higher-fidelity simulations could benefit from integrating LBM for complex geometries and AI-driven models for real-time analysis. Incorporating these advancements into hydrodynamic studies holds promise for advancing riverine engineering practices, particularly in flood management and navigational design.

REFERENCES

[1] Y. Shimizu, H. Yamaguchi, and T. Itakura, "Three-Dimensional Computation of Flow and Bed Deformation," *Journal of Hydraulic Engineering*, vol. 116, no. 9, pp. 1090–1108, Sep. 1990, https://doi.org/10.1061/(ASCE)0733-9429(1990)116:9(1090).

[2] P. M. Steffler and J. Yee-Chung, "Depth averaged and moment equations for moderately shallow free surface flow," *Journal of Hydraulic Research*, vol. 31, no. 1, pp. 5–17, Jan. 1993, https://doi.org/10.1080/00221689309498856.

[3] H. C. Lien, T. Y. Hsieh, J. C. Yang, and K. C. Yeh, "Bend-Flow Simulation Using 2D Depth-Averaged Model," *Journal of Hydraulic Engineering*, vol. 125, no. 10, pp. 1097–1108, Oct. 1999, https://doi.org/10.1061/(ASCE)0733-9429(1999)125:10(1097).

[4] H. Zobeyer and P. M. Steffler, "Modeling flow in curved open channel by a quasi-3D Model," in *River Flow 2010*, A. Dittrich, K. Koll, J. Aberle, and P. Geisenhainer, Eds. 2010, pp. 1535–1542.

[5] R. Nagaosa, "Direct numerical simulation of vortex structures and turbulent scalar transfer across a free surface in a fully developed turbulence," *Physics of Fluids*, vol. 11, no. 6, pp. 1581–1595, Jun. 1999, https://doi.org/10.1063/1.870020.

[6] V. Borue, S. A. Orszag, and I. Staroselsky, "Interaction of surface waves with turbulence: direct numerical simulations of turbulent open-channel flow," *Journal of Fluid Mechanics*, vol. 286, pp. 1–23, Mar. 1995, https://doi.org/10.1017/S0022112095000620.

[7] T. Kawamura, "Numerical simulation of 3D turbulent free surface flows," Ph.D. dissertation, University of Tokyo, Tokyo, Japan, 1998.

[8] F. P. Lugina, T. Uchida, and Y. Kawahara, "Numerical Calculations for Curved Open Channel Flows with Advanced Depth-Integrated Models," *KSCE Journal of Civil Engineering*, vol. 28, no. 3, pp. 1026–1040, Mar. 2024, https://doi.org/10.1007/s12205-024-1431-7.

[9] K. Onitsuka and I. Nezu, "Numerical Prediction of Rectangular Open-Channel Flow by Using Large Eddy Simulation," in *Proceedings of the 29th IAHR World Congress (Beijing, 2001)*, Beijing, China, 2001.

[10] L. Shen and D. K. P. Yue, "Large-eddy simulation of free-surface turbulence," *Journal of Fluid Mechanics*, vol. 440, pp. 75–116, Aug. 2001, https://doi.org/10.1017/S0022112001004669.

[11] T. G. Thomas, J. J. R. Williams, and D. C. Leslie, "Development of a conservative 3D free surface code," *Journal of Hydraulic Research*, vol. 30, no. 1, pp. 107–115, Jan. 1992, https://doi.org/10.1080/00221689209498950.

[12] J. Shi, T. G. Thomas, and J. J. R. Williams, "Free-Surface Effects in Open Channel Flow at Moderate Froude and Reynold's Numbers," *Journal of Hydraulic Research*, vol. 38, no. 6, pp. 465–474, Nov. 2000, https://doi.org/10.1080/00221680009498300.

[13] A. Nakayama and S. Yokojima, "Les of Open-Channel Flow with Free-Surface Fluctuation," *Proceedings of Hydraulic Engineering*, vol. 46, pp. 373–378, 2002, https://doi.org/10.2208/prohe.46.373.

[14] H.-C. Zheng, Z.-M. Shi, M. Peng, and S.-B. Yu, "Coupled CFD-DEM model for the direct numerical simulation of sediment bed erosion by viscous shear flow," *Engineering Geology*, vol. 245, pp. 309–321, Nov. 2018, https://doi.org/10.1016/j.enggeo.2018.09.003.

[15] M.-L. Zhang, C. W. Li, and Y.-M. Shen, "A 3D non-linear k–ε turbulent model for prediction of flow and mass transport in channel with vegetation," *Applied Mathematical Modelling*, vol. 34, no. 4, pp. 1021–1031, Apr. 2010, https://doi.org/10.1016/j.apm.2009.07.010.

[16] A. Gholami, H. Bonakdari, A. H. Zaji, and A. A. Akhtari, "A comparison of artificial intelligence-based classification techniques in predicting flow variables in sharp curved channels," *Engineering with Computers*, vol. 36, no. 1, pp. 295–324, Jan. 2020, https://doi.org/10.1007/s00366-018-00697-7.

[17] S. Kadia, L. Lia, I. Albayrak, and E. Pummer, "The effect of cross-sectional geometry on the high-speed narrow open channel flows: An updated Reynolds stress model study," *Computers & Fluids*, vol. 271, Mar. 2024, Art. no. 106184, https://doi.org/10.1016/j.compfluid.2024.106184.

[18] B. Malvandi and M. F. Maghrebi, "Prediction of boundary shear stress distribution in straight open channels using velocity distribution," *Water Science and Engineering*, vol. 14, no. 2, pp. 159–166, Jun. 2021, https://doi.org/10.1016/j.wse.2021.03.005.

[19] S. Moradi, K. Esmaili, and S. R. Khodashenas, "Experimental study on velocity distribution and bed load transport in compound channels: Effect of the floodplain's wall parallel with the meandering main channel," *Journal of Hydrology*, vol. 621, Jun. 2023, Art. no. 129571, https://doi.org/10.1016/j.jhydrol.2023.129571.

[20] H. Kakavandi, M. M. Heidari, and R. Ghobadian, "A numerical model for calculating velocity distribution in cross-section of an open channel," *Applied Water Science*, vol. 14, no. 3, Feb. 2024, Art. no. 37, https://doi.org/10.1007/s13201-023-02090-2.

[21] R. Absi, "An ordinary differential equation for velocity distribution and dip-phenomenon in open channel flows," *Journal of Hydraulic Research*, vol. 49, no. 1, pp. 82–89, Feb. 2011, https://doi.org/10.1080/00221686.2010.535700.

[22] F. Rooniyan, "The Effect of Confluence Angle on the Flow Pattern at a Rectangular Open-Channel," *Engineering, Technology & Applied Science Research*, vol. 4, no. 1, pp. 576–580, Feb. 2014, https://doi.org/10.48084/etasr.395.

[23] S. M. Kori, A. A. Mahessar, M. Channa, A. A. Memon, and A. R. Kori, "Study of Flow Characteristics Over a Rounded Edge Drop Structure in Open Channel," *Engineering, Technology & Applied Science Research*, vol. 9, no. 3, pp. 4136–4139, Jun. 2019, https://doi.org/10.48084/etasr.2584.

[24] F. P. Lugina, T. Uchida, and Y. Kawahara, "Numerical Calculations for Curved Open Channel Flows with Advanced Depth-Integrated Models," *KSCE Journal of Civil Engineering*, vol. 28, no. 3, pp. 1026–1040, Mar. 2024, https://doi.org/10.1007/s12205-024-1431-7.